Photodissociation and Recombination of Carbonmonoxy Cytochrome Oxidase: Dynamics from Picoseconds to Kiloseconds†

Ólöf Einarsdóttir,*,‡ R. Brian Dyer,§ Douglas D. Lemon,§ Patrick M. Killough,§,∥ Stephan M. Hubig,⊥ Stephen J. Atherton,⊥ Juan J. López-Garriga,§,# Graham Palmer,○ and William H. Woodruff*,§

Department of Chemistry, University of California, Santa Cruz, California 95064, Los Alamos National Laboratory, Los Alamos, New Mexico 87545, Center for Fast Kinetics Research, The University of Texas at Austin, Austin, Texas 78712, and Department of Biochemistry and Cell Biology, Rice University, Houston, Texas 77251

Received June 30, 1993®

ABSTRACT: The kinetics of the flash-induced photodissociation and rebinding of carbon monoxide in cytochrome aa_3–CO have been studied by time-resolved infrared (TRIR) and transient ultraviolet–visible (UV–vis) spectroscopy at room temperature and by Fourier transform infrared (FTIR) spectroscopy at low temperature. The binding of photodissociated CO to Cu_B^+ at room temperature is conclusively established by the TRIR absorption at 2061 cm^{-1} due to the C–O stretching mode of the Cu_B^+–CO complex. These measurements yield a first-order rate constant of $(4.7 \pm 0.6) \times 10^5\ s^{-1}$ ($t_{1/2} = 1.5 \pm 0.2\ \mu s$) for the dissociation of CO from the Cu_B^+–CO complex into solution. The rate of rebinding of flash-photodissociated CO to cytochrome a_3^{2+} exhibits saturation kinetics at [CO] > 1 mM due to a preequilibrium between CO in solution and the Cu_B^+–CO complex ($K_1 = 87\ M^{-1}$), followed by transfer of CO to cytochrome a_3^{2+} ($k_2 = 1030\ s^{-1}$). The CO transfer from Cu_B to Fe_{a_3} was followed by CO–FTIR between 158 and 179 K and by UV–vis at room temperature. The activation parameters over the temperature range 140–300 K are $\Delta H^\ddagger = 10.0$ kcal mol^{-1} and $\Delta S^\ddagger = -12.0$ cal $mol^{-1}\ K^{-1}$. The value of $\Delta H^\ddagger$ is temperature independent over this range; i.e., $\Delta C_p^\ddagger = 0$ for CO transfer. Rapid events following photodissociation and preceding rebinding of CO to cytochrome a_3^{2+} were observed. An increase in the α-band of cytochrome a_3 near 615 nm ($t_{1/2}$ ca. 6 ps) follows the initial femtosecond time-scale events accompanying photodissociation. Subsequently, a decrease is observed in the α-band absorbance ($t_{1/2} \sim 1\ \mu s$) to a value typical of unliganded cytochrome a_3. This latter absorbance change appears to occur simultaneously with the loss of CO by Cu_B^+. We ascribe these observations to structural changes at the cytochrome a_3 induced by the formation and dissociation of the Cu_B^+–CO complex. We suggest that the picosecond binding of photodissociated CO to Cu_B triggers the release of a ligand L from Cu_B. We infer that L then binds to cytochrome a_3 on the distal side and that this process is directly responsible for the observed α-band absorbance changes. We have previously suggested that the transfer of L produces a transient five-coordinate high-spin cytochrome a_3 species where the proximal histidine has been replaced by L. When CO binds to the enzyme from solution, these processes are reversed. The dissociation of L from the heme is suggested to be the rate-determining step for transfer of CO from its preequilibrium binding site on Cu_B to its thermodynamically stable binding site on the heme iron. These findings suggest an additional feature of the "ligand shuttle" role that we previously proposed for Cu_B in the functional dynamics of cytochrome oxidase. We suggest that the ligand shuttle may occur during the binding of other small molecules, most notably O_2, at the active site and that these ligand-exchange processes may represent a control and coupling mechanism for the electron-transfer and proton-translocation reactions of the enzyme.

Cytochrome oxidase (CcO; ferrocytochrome *c*:oxygen oxidoreductase, EC 1.9.3.1) is a complex integral protein present in the mitochondrial inner membrane of eukaryotes and the cell membrane of many prokaryotes. This enzyme catalyzes the reduction of dioxygen to water by cytochrome *c* [*cf.* Wikström et al. (1981) for review]. It contains two heme A chromophores (cytochromes *a* and a_3) and two redox-active copper centers (Cu_A and Cu_B) coordinated to the protein. In addition, the beef heart enzyme contains one zinc and one magnesium atom, both of unknown function (Einarsdóttir & Caughey, 1985). A third copper, of unknown significance, has also been suggested to be a component of the protein (Einarsdóttir & Caughey, 1985; Bombelka et al., 1986; Steffans et al., 1987) and may be integral with Cu_A in a binuclear two-copper site (Kronek et al., 1991). Under most functional conditions each heme/copper pair works as a unit. The magnetically isolated cytochrome *a* (Fe_a) and Cu_A centers, located near the outer surface of the mitochondrial membrane, accept electrons donated by reduced cytochrome *c* and transfer them to the site of O_2 reduction, which comprises cytochrome a_3 (Fe_{a_3}) and Cu_B. The latter two metal centers are in close enough proximity to one another (probably ≤5 Å; Babcock, 1988) to be antiferromagnetically coupled in oxidized forms of the enzyme.

While the binding of ligands to ferrous cytochrome a_3 has been known since the classical work of Keilin and Hartree (1938) and indeed is generally believed to be an obligatory

† This work was supported by National Institutes of Health Grants DK 36263 (W.H.W.), GM 21337 (G.P.), and RR 00886 (Center for Fast Kinetics Research). Work at Los Alamos National Laboratory was performed under the auspices of the U.S. Department of Energy.

* Authors to whom correspondence should be addressed.
‡ University of California.
§ Los Alamos National Laboratory.
∥ Present address: Shell Development Co., Houston, TX 77251.
⊥ Center for Fast Kinetics Research.
Present address: University of Puerto Rico, Mayagüez, PR 00708.
○ Rice University.

® Abstract published in *Advance ACS Abstracts,* September 1, 1993.

0006-2960/93/0432-12013$04.00/0

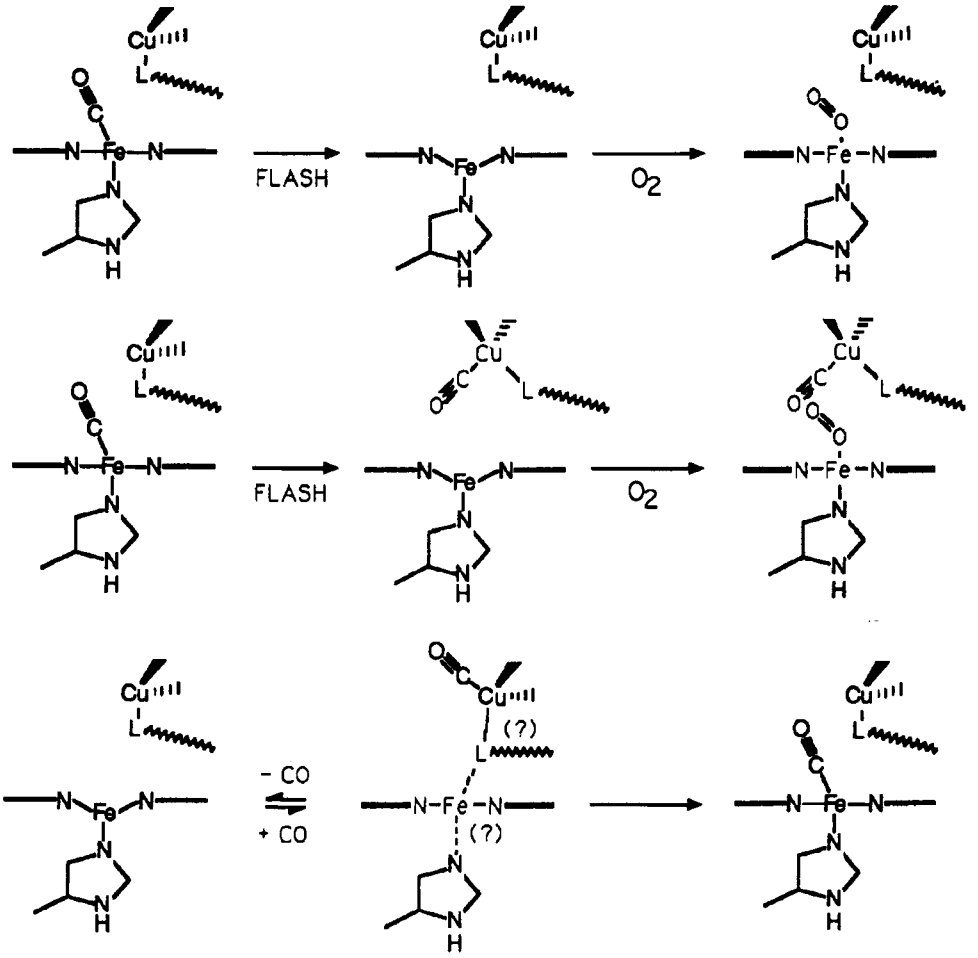

FIGURE 1: Schematic representations of ligation reactions at the binuclear site of cytochrome oxidase. Top: flow–flash reaction, assuming no interference from photodissociated CO. Middle: flow–flash reactions, assuming interference from Cu_B^+–CO. Bottom: generalized reaction for the binding of ligands (with CO as an example) to the binuclear site.

step preceding the reduction of dioxygen to water (Babcock et al., 1984; Chance et al., 1975; Gibson & Greenwood, 1963; Greenwood & Gibson, 1967; Hill et al., 1986), the binding of ligands to Cu_B has only recently been demonstrated. Currently it appears that both CO and NO can bind to the cuprous center (Alben et al., 1981; Fiamingo et al., 1982; Stevens et al., 1979; Boelens et al., 1984). Cyanide can bind to cupric or cuprous copper and ferric or ferrous cytochrome a_3, depending on the overall oxidation state of the enzyme (Yoshikawa & Caughey, 1990). Nevertheless, the binding of ligands to Cu_B has generally been assumed to have minimal functional significance compared to the well-established role of cytochrome a_3. The coordination chemistry of the cytochrome a_3/Cu_B pair and the dynamics of the ligand binding reactions are key features of the physiological function of the enzyme and also of inhibitory phenomena manifested as CO and CN-toxicity.

Due to the rapidity of the reaction of reduced cytochrome oxidase with dioxygen, this reaction is difficult to study by conventional rapid-mixing techniques (Gibson & Greenwood, 1963; Greenwood & Gibson, 1967; Hill et al., 1986; Wikström et al., 1981). Carbon monoxide, however, binds to ferrous cytochrome a_3 and forms a thermodynamically ($K_f = 3.3 \times 10^6\ M^{-1}$) (Yoshikawa et al., 1977) and kinetically ($t_{1/2} = 30$ s for dissociation; Greenwood & Gibson, 1967) stable complex with the reduced enzyme. Since CO and O_2 compete for the same binding site, the binding and reduction of O_2 is blocked in the CO complex as long as CO remains bound to $Fe_{a_3}^{2+}$. It was recognized by Gibson and Greenwood (1963) that photodissociation of CO from this inhibitor complex in the presence of O_2 allows the O_2 ligation and reduction reactions to be observed on a time scale approaching diffusion control rather than that of the mixing of the reactants. This elegant "flow–flash" approach and related trapping techiques which were subsequently developed have allowed investigation of the O_2 reactions in considerable detail and have provided significant information regarding the rates of internal electron-transfer processes and the possible structures of the transient intermediates that are generated in this reaction (Gibson & Greenwood, 1963; Greenwood & Gibson, 1967; Chance et al., 1975; Clore et al., 1980; Karlsson et al., 1981; Hill et al., 1986; Blackmore et al., 1991).

The relevance of the flow–flash and trapping experiments requires that photodissociated CO not interfere with the reaction with oxygen. This scenario is depicted in the top schematic of Figure 1. However, FTIR studies have demonstrated that photodissociated CO migrates to and binds to Cu_B in mitochondrial preparations under cryogenic conditions (Alben et al., 1981; Fiamingo et al., 1982). More recently, our FTIR studies of cytochrome ba_3 from the bacterium *Thermus thermophilus* have shown that photodissociated CO binds quantitatively to Cu_B^+ at temperatures between 20 and 300 K (Einarsdóttir et al., 1989). We have used time-resolved infrared (TRIR) spectroscopy to demonstrate that this also occurs as a microsecond time-scale transient at room temperature in the mammalian enzyme (Dyer et al., 1989a). Such a Cu_B^+–CO species might hinder O_2 binding to cytochrome a_3^{2+} (e.g., depicted in the middle schematic of Figure 1). It will clearly have redox characteristics which differ from the unliganded system. Quite recent results (Blackmore et al.,

1991) suggest that, at room temperature in mammalian CcO, this intermediate is too short-lived to compromise flow–flash studies. On the other hand, a preliminary report (Song et al., 1992) suggests that the products of the flow–flash reaction and those of the O_2 oxidation initiated by rapid mixing may differ. In any case, the following caveats must be kept in mind: Cu_B^+–CO will interfere with flow–flash studies of oxidases (such as cytochrome ba_3) which have a large Cu–CO binding constant (Einarsdóttir et al., 1989); and even if the binding constant is small, this complex may interfere with short time-scale or cryogenic measurements.

More fundamentally, however, the transient fate of the photodissociated CO and the kinetics of the formation and relaxation of the photoinduced transient intermediates become of crucial importance in establishing whether obligatory binding of CO and other small exogenous ligands, particularly O_2, to Cu_B is a general mechanistic feature of the dynamics of the enzyme. This is depicted in the bottom schematic of Figure 1, which shows CO (or, by implication, O_2, NO, RNC, etc.) binding to Cu_B on the pathway from solution to the thermodynamically stable binding site on $Fe_{a_3}^{2+}$. In addition, the possibility that the binding of exogenous ligands to Cu_B may trigger exchange of an endogenous ligand between Cu_B and Fe_{a_3} (perhaps with simultaneous cleavage of the proximal histidine bond) is depicted.

Here we report the results of a kinetics study of the events occurring on the picosecond to kilosecond time scale following the photolysis of CO from cytochrome a_3, including the fate of the photodissociated CO and the formation and relaxation of the transient intermediates. Our data support a preequilibrium between free CO in solution and a non-heme CO-bound transient intermediate prior to the formation of the cytochrome a_3–CO complex. The CO–FTIR flash-photolysis kinetic results at low temperature [as well as previous infrared studies on mitochondrial preparations (Alben et al., 1981; Fiamingo et al., 1982)] and TRIR studies of CcO–CO photodynamics at room temperature provide conclusive evidence that this intermediate is Cu_B^+–CO (Dyer et al., 1989a). Recent studies by others (Blackmore et al., 1991; Oliveberg & Malmström, 1992) strongly support our earlier suggestion (Dyer et al., 1989a; Woodruff et al., 1991a) that this preequilibrium also occurs in the reaction with O_2, prior to O_2 binding at the heme. This observation validates our view that the CO results are relevant to the functional reactions of the enzyme. Our transient UV–vis results suggest that the binding of CO to Cu_B^+ may cause a ligand (hereinafter denoted L) to be exchanged between Cu_B and Fe_{a_3}. Recent time-resolved resonance Raman (TR^3) and time-resolved magnetic circular dichroism (TRMCD) evidence from our laboratories suggests that this may occur with the simultaneous release and rebinding of the proximal histidine as suggested by Figure 1 (Woodruff et al., 1991a; Goldbeck et al., 1991). This raises the intriguing possibility that Cu_B assumes a previously unsuspected role as the gateway to the active site, affecting ligand and substrate transport in the functional dynamics of cytochrome oxidases. These results suggest new possibilities for the microscopic mechanism of the reduction of dioxygen to water catalyzed by cytochrome oxidase. We speculate that the binding of O_2 to Cu_B and the concomitant exchange of L between Cu_B and cytochrome a_3 may have a functional role in gating proton translocation and electron transfer, and perhaps coupling the two, within the enzyme.

MATERIALS AND METHODS

Cytochrome oxidase was isolated from fresh bovine heart muscle by the following modification of published methods (Yoshikawa et al., 1977). Following the last fractionation between 25% and 35% ammonium sulfate in 0.5% cholate, the precipitate was dissolved in 200 mL of 0.1 M sodium phosphate buffer, pH 7.4, containing 0.75% dodecyl maltoside [0.75% Tween-20 in preparation A (Yoshikawa et al., 1977)]. The enzyme solution was adjusted to 25% ammonium sulfate and centrifuged for 10 min at 17 000 rpm. The resulting supernatant was adjusted to 50% ammonium sulfate to precipitate the contaminant cytochrome *b*. The oxidase was precipitated out at 60% ammonium sulfate. This precipitate in 0.75% dodecyl maltoside was subjected to an additional three fractionations between 25% and 35% ammonium sulfate in 0.5% cholate. The final precipitate from these fractionations was dissolved in 10 mM sodium phosphate buffer containing 0.1% dodecyl maltoside, pH 7.4, and dialyzed against the same buffer overnight at 4 °C. The purified oxidase was concentrated to ~2.0 mM in heme A in an Amicon Diaflow apparatus. The yield from this method is high, and the product is unusually soluble and fluid at high concentrations. Cytochrome oxidase was also prepared by the aforementioned method (Yoshikawa et al., 1977) with Brij 35 substituted for Tween-20. Cytochrome oxidase prepared by a modified procedure of Hartzell and Beinert (Baker et al., 1987) was used for selected CO-binding kinetics studies of cytochrome a_3 as a function of CO pressure. This preparation was solubilized in 0.1 M sodium phosphate buffer containing 0.1% dodecyl maltoside, pH 8.0. Results from the three preparations were indistinguishable.

Fully reduced cytochrome oxidase was obtained by deoxygenating the oxidized, resting enzyme by alternating cycles of vacuum and N_2 gas, followed by the addition of a small excess of dithionite. The fully reduced CO-bound IR (FTIR and TRIR) samples were obtained by passing CO over a solution of fully reduced enzyme for 60–90 min. The IR samples, ~2.0 mM in heme A, were pressed between a pair of round sapphire or CaF_2 windows (0.05-mm optical path length) under a CO atmosphere. The UV–vis spectrum of the CO complex in the IR cell was recorded before and after the FTIR and TRIR spectral measurements on a Cary 14 spectrophotometer to verify the sample integrity and to ensure that no spectral changes had occurred during the course of the infrared experiments.

The CO–FTIR spectra were recorded on a Digilab FTS-40 Fourier transform infrared (FTIR) spectrometer. Low temperatures were achieved with an Air Products Displex closed-cycle helium refrigerator. Interferograms were collected at 1-cm^{-1} resolution in a single-beam mode. The single-beam dark spectra were recorded before photolysis and the low-temperature single-beam light spectra after a few minutes exposure from a 500-W tungsten lamp, or after irradiation by all lines of the blue-green output of a Spectra-Physics 171 continuous-wave Ar^+ laser at approximately 4-W total power. The single-beam light and dark spectra each represent an average of 1024 interferograms. The kinetics of the thermal dissociation of CO from Cu_B^+ and its rebinding to the cytochrome a_3^{2+} were followed by FTIR between 158 and 179 K. The kinetic time-dependent infrared spectra are an average of between 16 and 64 interferograms, depending on the rate of the return of the photolyzed state to equilibrium. The time for data collection was kept short compared to the time required for the rebinding of the photodissociated CO to the cytochrome a_3^{2+}. Between the kinetics runs at various temperatures from 158 to 179 K the CO was allowed to relax back to the cytochrome a_3 in the dark at 210 K for 15–30 min.

The TRIR experiments were carried out using the approaches described previously (Dyer et al., 1989a). The sample

was probed with a Laser Analytics continuous-wave diode laser. A diode which was tunable between 2040 and 2080 cm^{-1} was used to observe the C–O stretch of the Cu–CO complex, and the heme-bound CO was observed with a diode tunable between 1940 and 1990 cm^{-1}. The diode laser produced approximately 1-mW multimode output. Dissociation of CO was initiated with 7-ns second harmonics pulses from a Quanta-Ray DCR-1A Nd:YAG laser (532 nm, 20 mJ/pulse) operated at a repetititon rate of 10 Hz. The 100-ms pulse interval allowed re-formation of the starting aa_3–CO complex between pulses ($t_{1/2}$ ca. 10 ms for recombination at 1 atm of CO). Further experimental details have been described previously (Dyer et al., 1989a).

The room temperature flash photodissociation–rebinding studies of cytochrome aa_3–CO were carried out by kinetic spectrophotometry at the Center for Fast Kinetics Research (CFKR), The University of Texas at Austin. A vacuum line equipped with a gas reservoir and side arms for gas inlet and sample cuvette attachment was used to manipulate the CO pressure. The reduced sample was prepared by repeated evacuation/N_2 cycles followed by the addition of a small excess of dithionite. Gas pressures in this line were measured using a MKS Barytron pressure transducer and gauge. Below 1 atm of CO the line and gas reservoir were evacuated and filled to a desired pressure of CO. Subsequently, N_2 was added to give a final pressure of 1000 Torr, and the gas reservoir was then closed off from the rest of the line. Following the evacuation of the gas line, the gas mixture from the reservoir was bled into the vacuum line to a pressure of ~760 Torr. The sample cuvette was then opened, and the final gas pressure was adjusted to 744 Torr (ambient pressure in Austin, Texas). CO pressures above atmospheric were established directly by the gauge reading [from 5 to 330 psig (20 to 345 psia) inclusively], with no N_2 diluent. The lower regulator gauge pressures were checked for accuracy with the Barytron gauge until the pressure range of this device was exceeded. At gas pressures above 30 psig a special high-pressure cell was employed which consisted of a Pyrex tube 8 mm o.d. by 2 mm i.d., sealed on one end and connected to a stainless steel tube by a glass-to-metal seal on the other. This was connected via a stainless steel bellows valve to a Swagelok fitting for attachment to the gas regulator and cylinder. For the variable CO concentration experiments, the reduced enzyme (10 μM in heme A) was equilibrated with the desired gas mixture CO/N_2 at room temperature for a few minutes prior to spectral measurement. Other transient absorption measurement were carried out at 1 atm of CO unless stated otherwise. Transient absorbance difference spectra and single-wavelength kinetic measurements were made using a Quantel YG481 Nd:Yag laser and associated kinetic spectrophotometer. The second harmonic (532 nm, ca. 12 ns) pulse was used as an excitation source. For time scales less than 200 μs, a 150-W xenon arc lamp was used as a monitoring source, while for longer times, a 12-V tungsten lamp gave greater stability. Signals were fed to a Biomation 8100 transient digitizer and then to a DEC PDP11/70 minicomputer for analysis. The rebinding of the photodissociated CO to the cytochrome a_3 iron as a function of CO concentration was monitored by the light absorption at 443 nm (the absorption maximum of the fully reduced unliganded enzyme), whereas the nanosecond–microsecond kinetics were followed both at 610 nm (55 μM in heme A) and at 443 nm (10 μM in heme A). The picosecond experiments were carried out using an apparatus described previously (Atherton et al., 1987). A mode-locked Nd:YAG laser providing 532-nm pulses of 30-ps duration was used as an excitation source, and data were collected and analyzed using a microcomputer.

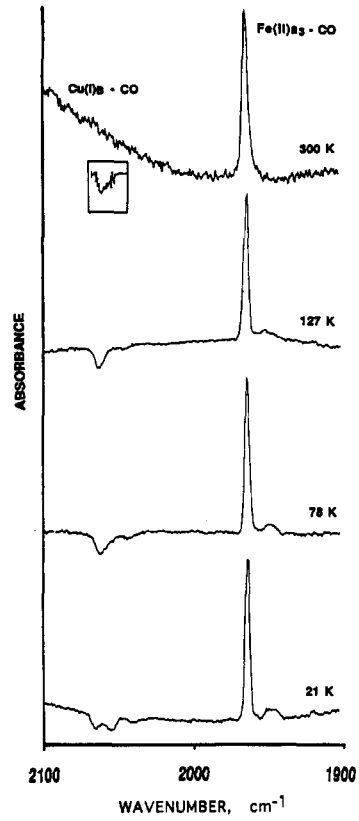

FIGURE 2: FTIR difference spectra (unphotodissociated minus photodissociated) of CO–cytochrome oxidase, taken in the C–O stretching region of the IR spectrum at temperatures as indicated; see text for details. Inset on 300 K trace: point-by-point TRIR spectrum of the Cu_B–CO region at 300 K with absorbance change at 500 ns after photodissociation. The vertical error bars represent the standard deviations of repeated TRIR experiments at each IR frequency.

RESULTS

We have studied the photodissociation and recombination reactions of the carbon monoxide complex of fully reduced beef heart cytochrome oxidase on picosecond and longer time scales. We present the Results section of this report organized as to the spectroscopic technique employed in monitoring the reaction. In the Discussion section we will present our interpretation of these results more generally in terms of the physical events occurring during the different time scales.

CO–FTIR. Alben and co-workers originally established by CO–FTIR on mitochondrial preparations (Alben et al., 1981; Fiamingo et al., 1982; Fager & Alben, 1972) that when CO is photolyzed from the ferrous cytochrome a_3 of bovine cytochrome oxidase, it binds to Cu_B^+ at temperatures up to 180 K. This is verified here using the purified enzyme. Figure 2 shows the dark (before photolysis) minus light (after photolysis) CO–FTIR difference spectra as a function of temperature. The peaks at 1963 and 1948 cm^{-1} at low temperatures and at 1963 and 1959 cm^{-1} at room temperature correspond to CO bound to the ferrous cytochrome a_3, whereas the troughs found at 2062, 2054 (at 25 K), and 2048 cm^{-1} are due to CO bound to Cu_B^+. Below 180 K the photodissociated spectra could be recorded on the time scale required to obtain a FTIR spectrum, subsequent to illumination; at 300 K the photodissociation was accomplished by continuous laser illumination. For reasons which will be discussed below the Cu_B^+C–O trough is not observed in the room temperature photostationary FTIR spectrum but is detected by TRIR (*vide infra*) and is shown in the inset of Figure 2.

The observed FeC–O and CuC–O frequencies and bandwidths are similar to those observed for CO bound to bovine heart mitochondria photolyzed at low temperatures (Alben et al., 1981; Fiamingo et al., 1982). The ν_{CO} due to CO bound to cytochrome a_3 determined at room temperature (top panel) is in good agreement with previous CO–IR studies of CO bound to fully reduced enzyme (Yoshikawa & Caughey, 1982; Einarsdóttir et al., 1988). The narrow bandwidths, $\Delta\nu_{1/2} \sim 4$ and 8 cm^{-1} for the FeC–O peak and CuC–O trough, respectively, reinforce the previous suggestion (Fiamingo et al., 1982; Yoshikawa & Caughey, 1982; Einarsdóttir et al., 1988) of a unique orientation of bound CO relative to the protein structure and a relatively homogeneous and inflexible environment around the CO at both metal centers. The multiple frequencies of the FeC–O and CuC–O bands are generally believed to represent discrete conformers of CcO (Yoshikawa & Caughey, 1982; Einarsdóttir et al., 1988). This conformational effect on heme C–O frequencies has been observed in the carbonyl complexes of many heme proteins (Caughey, 1980; Choc & Caughey, 1981; Shimada & Caughey, 1981).

The integrated absorptivities for CO bound to heme and copper proteins are linearly correlated with the C–O stretching frequency (Alben et al., 1981). We have applied this relationship to our data and find that the relative areas of the FeC–O and CuC–O absorbance below 180 K represent quantitative transfer of CO from heme to copper upon photodissociation. This result, and the quantitative recovery of the Fe–CO complex following relaxation of the Cu–CO complex at low temperature, is in agreement with the data of Alben and co-workers (Alben et al., 1981; Fiamingo et al., 1982). This observation supports the conclusion stated above, which is drawn from the line-widths values, of a closed heme–copper pocket, substantially isolated from the outside medium. This isolation and homogeneity of the heme–ligand binding site in cytochrome oxidase has been noted previously (Yoshikawa & Caughey, 1982; Einarsdóttir et al., 1988).

The photoinduced transfer of CO from the ferrous cytochrome a_3 to the copper is kinetically reversible above 140 K, but below this temperature the rate of the rebinding of CO to the heme becomes too slow to measure. Likewise, the rebinding process becomes too fast to follow reliably by FITR above 180 K. Between 158 and 179 K we followed the rates of the recombination by measuring the total area of the FeC–O and the CuC–O FTIR bands as a function of time after the photolyzing light had been turned off. The relaxation data were fit by a single exponential giving rate constants from 6.5×10^{-5} s^{-1} ($t_{1/2} \sim 180$ min) at 158 K to 4.4×10^{-3} s^{-1} ($t_{1/2} \sim 3$ min) at 179 K. No differences were observed between the kinetics determined using the area of the FeC–O absorbance on the one hand and the area of the CuC–O absorbance on the other, at any temperature. In agreement with the previous work on mitochondria (Fiamingo et al., 1982), we find that the kinetic data deviate somewhat from first-order behavior, but we made no attempt to obtain a better fit using multiple exponentials (Sharrock & Yonetani, 1977) or a distributed kinetics model (Fiamingo et al., 1982; Austin et al., 1975) because we were primarily interested in a semiquantitative characterization of the process.

Above 180 K the rebinding of the photodissociated CO to $Fe_{a_3}^{2+}$ is too rapid for observation of either the Cu–CO complex or the rebinding reaction by conventional FTIR kinetics measurements. We have observed Cu_B^+–CO at room temperature in cytochrome ba_3 (Einarsdóttir et al., 1989), using photostationary laser illumination at high intensity simultaneously with observation of the FTIR spectrum. This result

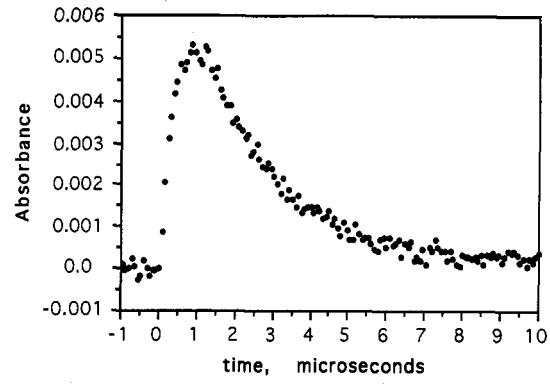

FIGURE 3: Post-photodissociation TRIR transient absorbance trace taken at the maximum of the Cu_B–CO absorbance peak, 2062 cm^{-1}.

suggested that a similar experiment might succeed with cytochrome aa_3. However, Cu_B^+–CO is not observed in cytochrome aa_3 using this approach (Figure 2, 300 K trace). This could be either because the equilibrium constant for the photostationary formation of Cu_B–CO is small at this temperature or because the Cu_B^+–CO complex simply does not form in the bovine enzyme except as an artifact of cryogenic conditions. In fact, we have observered the Cu_B^+–CO infrared transient at room temperature by kinetic TRIR (Dyer et al., 1989a; see below) and find that photostationary steady-state detection of this complex, which is possible in cytochrome ba_3 because of the kinetics and the equilibria involved, is very difficult in cytochrome aa_3 because the equilibrium concentration of Cu_B^+–CO at 1 atm of CO is small in the bovine enzyme.

TRIR. We have recently reported preliminary TRIR results on CO photodissociation and rebinding in cytochrome aa_3 on time scales down to 200 ns (Dyer et al., 1989a). More recent TRIR studies (Dyer et al., 1991) have followed post-photodissociation events with picosecond time resolution. In the present work, the dynamics of photodissociated CO were observed by following the transient infrared absorption at the C–O stretching frequency of the major Cu_B^+–CO absorption, 2062 cm^{-1} (present work and Fiamingo et al., 1982), and at the $Fe_{a_3}^{2+}$ C–O frequency, 1963 cm^{-1}. The transient kinetic response at 2062 cm^{-1} following photolysis at room temperature clearly shows the binding of photodissociated CO to Cu_B^+ (with an instrumentally limited apparent rise time of 200 ns) and the subsequent decay of the complex to form the unliganded protein and free CO (Figure 3). Picosecond TRIR measurements reported elsewhere show the rise time of Cu_B–CO following photodissociation to be less than 1 ps (Dyer et al., 1991). The first-order rate constant for the decay is $(4.7 \pm 0.6) \times 10^5$ s^{-1} ($t_{1/2} = 1.5 \pm 0.2$ μs). Identical results were obtained in glycerol (50% v/v) and non-glycerol-containing enzyme solutions. Figure 2 (inset in room temperature trace) shows the Cu_B^+–CO transient absorbance generated by observing the kinetic response at various frequencies within the Cu_B^+–CO absorption envelope. These data demonstrate conclusively that (i) the 2062-cm^{-1} transient is due to CO binding to Cu_B^+ and (ii) the major IR absorption of Cu_B^+–CO changes very little between 130 and 300 K, while the minor peak shifts from 2042 to 2052 cm^{-1} over this temperature range. The subsequent formation of the thermodynamically stable $Fe_{a_3}^{2+}$–CO complex can be observed by following the TRIR transient at 1963 cm^{-1}, which reveals that the recombination of CO with $Fe_{a_3}^{2+}$ occurs on a much slower time scale, having an observed rate constant of 91 s^{-1} at 1 atm of CO (Figure 4). Time-resolved infrared linear dichroism results reported elsewhere (Dyer et al., 1989b) show the angle between

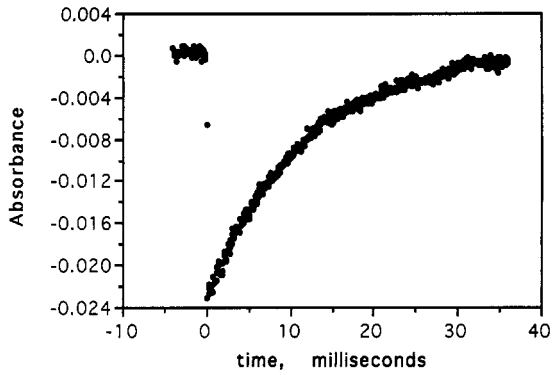

FIGURE 4: Post-photodissociation TRIR transient absorbance trace taken at the maximum of the Fe_{a_3}–CO absorbance peak, 1963 cm^{-1}.

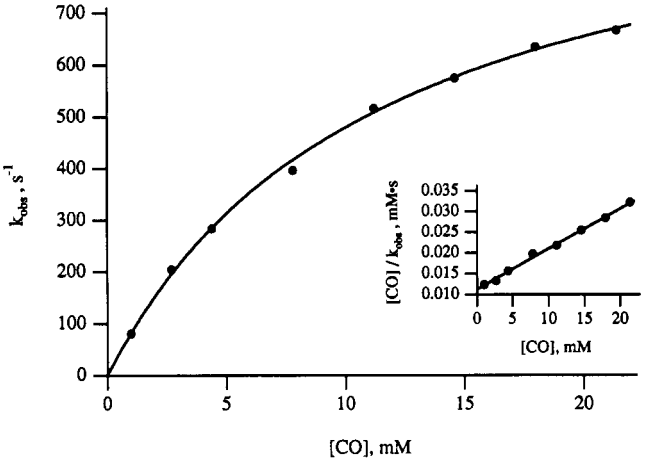

FIGURE 5: Saturation kinetics plot of the observed rate constant for rebinding of CO to Fe_{a_3} versus CO concentration. Inset: plot of the saturation kinetics data according to eq 6. See text.

the heme normal and the C–O bond vector to be 21° for $Fe_{a_3}^{2+}$–CO and 51° for Cu_B^+–CO.

Transient UV–vis Kinetics. The infrared kinetics measurements have great structural specificity and allow us to follow species such as Cu_B^+–CO which are inaccessible to other spectroscopic probes. However, transient UV–vis measurements are often more convenient for observing dynamics which affect the heme absorption spectrum and generally allow the observation of shorter time-scale events. We have employed two approaches to the UV–vis dynamics measurements, depending upon the time scale of interest: optical delay measurements using various mode-locked laser techniques which are suitable for studying the time window from 100 fs to a few nanoseconds and real-time measurements using Q-switched Nd:YAG laser photodissociation which are applicable to phenomena with lifetimes of ca. 10 ns or longer. The kinetics of the rebinding of flash-photodissociation CO to ferrous cytochrome a_3 were followed at room temperature by observing the transient absorbance changes at 443 nm (the Soret maximum for the unliganded cytochrome a_3) on a micro- and millisecond time scale. The observed first-order rate constant, k_{obs}, for CO rebinding to Fe_{a_3} in the presence of excess CO is approximately linearly dependent upon carbon monoxide concentration up to ~1 mM (P_{CO} ~ 1 atm) but shows the onset of saturation kinetics when [CO] exceeds 1 mM (P_{CO} ~ 1–22 atm; Figure 5). The value of k_{obs} was also found to be somewhat dependent on the light intensity of the white-light probe beam of the kinetic spectrophotometer. For example, at 1 atm of CO, increasing the power of the probe beam from 10 to 800 μW increases k_{obs} from 84 to 108 s^{-1}. This photoacceleration of the formation of the Fe–CO complex,

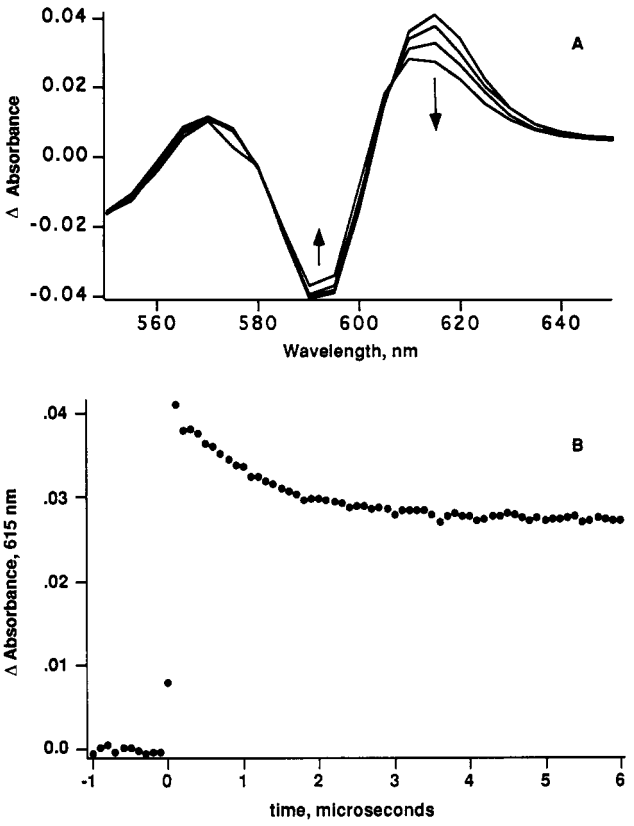

FIGURE 6: (A) Transient absorbance difference spectra in the α-band region of CO–cytochrome oxidase, taken between 100 ns and 5.4 μs of photodissociation. (B) Kinetics trace at 615 nm, corresponding to the spectra in (A).

which is itself photolabile, is at first surprising. This becomes important in understanding the detailed mechanism of ligand binding to cytochrome a_3 (*vide infra*).

Figure 6 shows the transient absorption difference spectrum in the α–β region of the heme spectrum between 540 and 700 nm, recorded between 100 ns and 5.4 μs after photolysis of CO from the cytochrome a_3. The decrease in absorbance intensity of the positive difference feature at wavelengths typical of unliganded cytochrome a_3 (ca. 615 nm) is obvious on this time scale. A half-life of 0.9 μs, corresponding to a first-order rate constant of 7.9×10^5 s^{-1}, is observed when the transient absorbance is monitored (absorbance decrease by approximately 25%; Figure 6B) on the nano/microsecond time scale. Other UV–vis features, notably the Soret difference spectrum, exhibit only very small changes during this time.

On the picosecond time scale an increase in intensity of the positive α-band difference near 615 nm is observed subsequent to the prompt (≤100 fs, *vide infra*) changes which occur upon CO photolysis from the cytochrome a_3. These changes in α-band intensity are accompanied by a significant shift of the α-band difference peak from 617 to 612 nm (Figure 7). As is the case with the nanosecond and microsecond data, only small changes are observed in the Soret difference spectrum after the initial absorbance jump during the laser pulse. Kinetic analysis of the α-band transient gives $t_{1/2}$ ~ 6 ps for these absorbance changes (Stoutland et al., 1991). These changes clearly are kinetically distinct from the prompt α-band absorbance increment and also the immediate changes in the Soret region (the latter register no additional changes between 10 ps and 1.5 ns. The prompt changes are due to the loss of CO by cytochrome a_3 which we have shown to occur in ≤100 fs (Stoutland et al., 1991); the subsequent (~6 ps) changes in the α-band intensity will be dealt with in the Discussion.

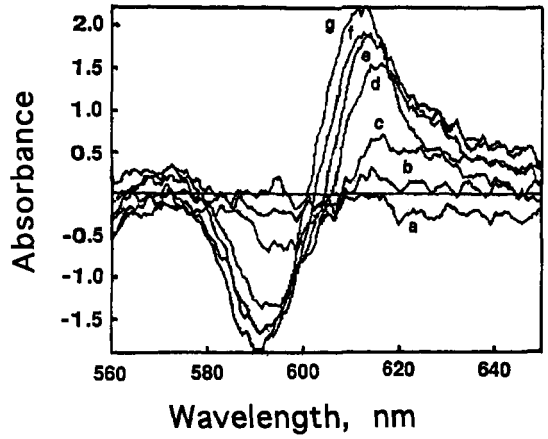

FIGURE 7: Picosecond transient absorbance difference spectra (nominal pulse duration of 25 ps) in the α-band region of CO–cytochrome oxidase. Times of arrival of the probe pulse at the sample prior to (negative numbers) and after (positive numbers) the photodissociation pulse are as follows: (a) −23 ps; (b) −17 ps; (c) −10 ps; (d) +3 ps; (e) +10 ps; (f) +17 ps; (g) +50 ps. The apparent absorbance changes are a convolution of the temporal characteristics of the photodissociation and probe pulses with the reaction dynamics. The reaction dynamics were ascertained by deconvolution techniques and also by independent experiments using subpicosecond pulses (Stoutland et al., 1991).

Scheme I

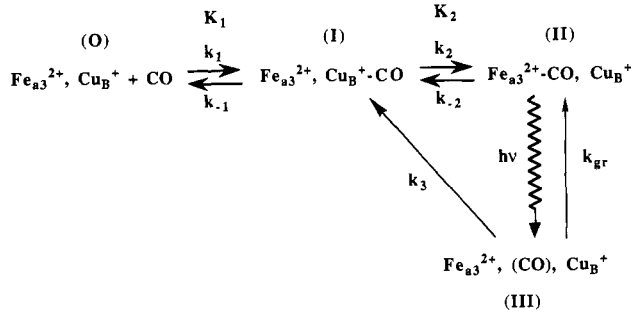

DISCUSSION

The general features of the CO rebinding kinetics observed by transient UV–vis absorbance, and also the time-resolved infrared results, can be explained by the kinetics model of the mechanism of the photodissociation and recombination of carbonmonoxy cytochrome oxidase shown in Scheme I. As we shall see, however, this model does not account for certain details. In Scheme I k_1 represents the binding of CO to Cu_B and k_2 its subsequent transfer to Fe_{a_3}; k_{-1} and k_{-2} are the reverse of these processes; $K_1 = k_1/k_{-1}$ and $K_2 = k_2/k_{-2}$; k_3 represents the formation of the Cu_B^+–CO complex (**I**) from the geminate photoproduct **III** formed in ≤100 fs (Stoutland et al., 1991); and k_{gr} represents the rate constant for geminate recombination of photodissociated CO with the heme. Scheme I assumes *a priori* a rapid preequilibrium (represented by K_1) between **I** and CO in solution. When this preequilibration is rapid relative to all of the other processes following the exceptionally fast formation of **I** from **III** ($k > 7 \times 10^{11}$ s^{-1}; Dyer et al., 1991), the observation of the re-formation of **II** following flash photodissociation will be kinetically identical with direct formation of **II** from the unliganded enzyme and CO in solution (as observed, for example, in a rapid mixing experiment). The validity of these assumptions can be verified after the relevant rate constants are determined, and this is discussed below. In Scheme I the formation of the Cu_B^+–CO complex is followed by the rate-determining step, the transfer of CO from Cu_B^+ to cytochrome a_3, represented by k_2. The rate constant for dissociation of CO from cytochrome a_3, k_{-2}, is 0.023 s^{-1} (Greenwood & Gibson, 1967), and this rate constant is much smaller than those of the other steps in the scheme. Provided that $k_{-1} \gg k_2$, the recombination rate law is[1]

$$\frac{d[\text{Fe–CO,Cu}]}{dt} = V = k_2[\text{Fe,Cu–CO}] = k_2K_1[\text{Fe,Cu}][\text{CO}] = k_{obs}[\text{Fe,Cu}]_T \quad (1)$$

The observed rate constant, k_{obs}, is[1]

$$k_{obs} = k_2\frac{[\text{CO}]}{[\text{CO}] + 1/K_1} \quad (2)$$

When $[\text{CO}] \ll 1/K_1$ (i.e., under nonsaturation conditions), $[\text{Fe,Cu}]_T \approx [\text{Fe,Cu}]$ and accordingly

$$\frac{d[\text{Fe–CO,Cu}]}{dt} \approx k_2K_1[\text{CO}][\text{Fe,Cu}]_T \quad (3)$$

As [CO] approaches or exceeds $1/K_1$, the onset of saturation behavior is observed, and ultimately, at high [CO], $[\text{Fe,Cu}]_T \approx [\text{Fe,Cu-CO}]$ and

$$\frac{d[\text{Fe–CO,Cu}]}{dt} \approx k_2[\text{Fe,Cu}]_T \quad (4)$$

Equation 2 predicts a hyperbolic dependence of k_{obs} on [CO], and thus at sufficiently high [CO], in the limit of full formation of Fe,Cu–CO, the maximum rate becomes independent of CO concentration as indicated in eq 4. This saturation behavior has not been observed previously in studies of CO rebinding to CcO, but as we shall see, this is simply because the small magnitude of K_1 makes it necessary to use pressures of CO above 1 atm to observe saturation. The conventional reciprocal form of eq 2 yields a linear relationship between $1/k_{obs}$ and $1/[\text{CO}]$, from which k_2 and K_1 can be determined (eq 5). Alternatively, eq 2 can be rearranged to yield eq 6,

$$\frac{1}{k_{obs}} = \frac{1}{k_2} + \frac{1}{k_2K_1}\frac{1}{[\text{CO}]} \quad (5)$$

whence $[\text{CO}]/k_{obs}$ and [CO] are linearly related, and once again, k_2 and K_1 can be determined. Equation 6 leads to plots that are linear rather than reciprocal in [CO], and this relationship will be used here.

$$\frac{[\text{CO}]}{k_{obs}} = \frac{[\text{CO}]}{k_2} + \frac{1}{k_2K_1} \quad (6)$$

Reaction Occurring within the Picosecond Time Scale. The photodissociation, migration, and binding of CO to Cu_B^+ (i.e., **II** → **III** → **I**) is quantitative and fast. The loss of CO by $Fe_{a_3}^{2+}$ occurs in less than 100 fs (Stoutland et al., 1991). By comparison, the vibrational period of the Fe–C bond is 64 fs. Rapid migration and binding to Cu_B were implied both by the original low-temperature CO–FTIR data on mitochondria (Fiamingo et al., 1982) and by our present CO–FTIR results which show that even at 20 K all of the photodissociated CO binds to copper in seconds or less, because the formation is complete in the minimum time required for conventional FTIR measurements. The conversion of **III** → **I** is responsible for the initial jump in the Cu_B^+–CO infrared transient at 2062 cm^{-1} (Figure 3). The time scale of the apparent rise of this absorbance in Figure 3 is equal to the response time of our real-time instrumentation, ~200 ns, so the formation of

[1] In these equations Fe and Cu represent $Fe_{a_3}^{2+}$ and Cu_B^+, respectively; Fe,Cu represents unliganded enzyme; Fe–CO,Cu and Fe,Cu–CO represent the respective CO–ligand derivatives; and $[\text{Fe,Cu}]_T$ represents [Fe,Cu] plus [Fe,Cu–Cu].

Cu_B^+–CO must be faster still. Quite recent picosecond TRIR results show the actual rise time to be astonishingly fast, less than 1 ps, yielding $k_3 > 7 \times 10^{11}$ s^{-1} (Dyer et al., 1991). This explains the observation (Gibson & Greenwood, 1963; Greenwood & Gibson, 1967; Findsen et al., 1987; confirmed in the present work) that photodissociated CO does not undergo geminate recombination with $Fe_{a_3}^{2+}$ to any detectable extent. Typical geminate recombination reactions in heme proteins occur on the nanosecond time scale (Martin et al., 1983). Thus it is reasonable that in CcO-photodissociated CO binds quantitatively to Cu_B^+ under simple kinetic control ($k_3 \gg k_{gr}$). The picosecond TRIR results suggest that there are no activation barriers of any sort to the migration of CO to Cu_B^+. It is clear that the enzyme is elegantly designed to facilitate ligand exchange between these two metal sites. The increase in intensity of the α-band of photodissociated cytochrome a_3 observed ca. 6 ps after CO photolysis is thus too slow to result directly from the binding of CO to Cu_B^+. In addition, binding of CO to Cu_B^+ should exert no direct effect upon the heme electronic absorbance. While the heme absorbance change and CO binding to Cu_B^+ are sequentially related, it appears that the formation of Cu_B^+–CO may only trigger a more direct effect on the heme structure which in turn is the proximate cause of the absorbance change.

Reactions Occurring on the Microsecond Time Scale. Our TRIR kinetics results show that the CO dissociates from the Cu_B^+ within microseconds ($k_{-1} = 4.7 \times 10^5$ s^{-1}, $t_{1/2} = 1.5$ μs under the conditions of the TRIR experiments) and equilibrates with CO in solution (Figure 3). On the same time scale ($k = 7.9 \times 10^5$ s^{-1}, $t_{1/2} \sim 0.9$ μs under the conditions of the UV–vis experiments) the intensity of the α-band of unliganded cytochrome a_3 decreases by approximately 25% (Figure 6). It is probable that the TRIR and UV–vis rate constants are experimentally the same and that differences in conditions, such as enzyme concentration (50 μM for the UV–vis kinetics experiments vs 1 mM for the TRIR) and solvent (50% glycerol solution vs aqueous buffer), account for the differences in the rate constants measured by the two approaches. Since the microsecond UV–vis absorbance changes occur on the same time scale as the CO dissociation from Cu_B established by the TRIR approach, this absorbance transient is probably due to changes occurring at cytochrome a_3 induced by dissociation of CO from Cu_B^+. As is the case in the picosecond results cited above, the ligation or deligation of Cu_B by CO is related in time to heme absorbance changes. It appears that these absorbance changes are triggered by, but not directly due to, the loss of CO by Cu_B in the reverse of the (as yet unspecified) process invoked above for the picosecond absorbance changes.

Reactions Occurring on the Millisecond Time Scale. The rebinding of photodissociated CO to cytochrome a_3 studied by transient absorption spectroscopy at room temperature displays the onset of saturation kinetics as CO pressure is raised above 1 atm (Figure 5). This behavior supports the suggestion in Scheme I that CO in solution reacts in a preequilibrium with a non-heme binding site prior to formation of the $Fe_{a_3}^{2+}$–CO complex. The microsecond time-scale TRIR data discussed above demonstrate unequivocally that this intermediate binding site is Cu_B^+. Furthermore, we have established the value of k_{-1} directly by TRIR (at high enzyme concentration in 50% glycerol) and have inferred its value from transient UV–vis (at low enzyme concentration in aqueous buffer). Equation 6 derived for Scheme I can be used to determine K_1 and k_2, whence the remaining rate and equilibrium constants can be estimated. A plot of $[CO]/k_{obs}$ versus [CO] (eq 6) is linear and yields values of 1030 s^{-1} and 87 M^{-1} for k_2 and K_1, respectively (Figure 5, inset). From

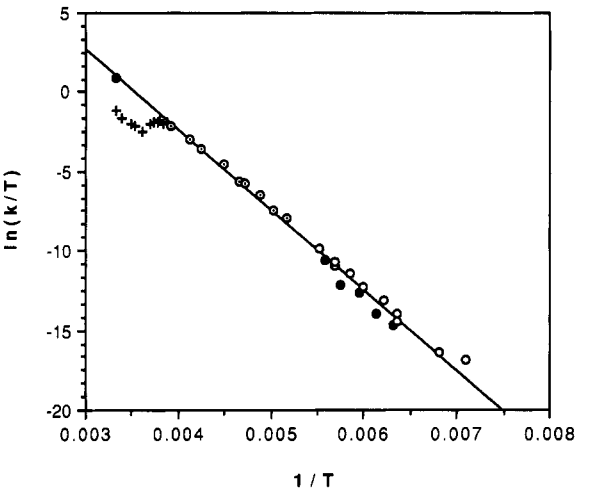

FIGURE 8: Eyring plot for the activation parameters associated with the transfer of CO from Cu_B to Fe_{a_3} in the rebinding reaction of CO–cytochrome oxidase. Symbols: filled circles, present work; open circles, Fiamingo et al. (1982); crosses and circles with concentric dots, Sharrock and Yonetani (1977). See text.

K_1 and k_{-1} (the latter from the UV–vis data, *vide supra*) the formation rate constant k_1 for Cu_B^+–CO is calculated as 6.8×10^7 M^{-1} s^{-1}.

The previously reported dissociation constant of CO from fully reduced oxidase, K_d, is 300 nM (Yoshikawa et al., 1977). In the context of Scheme I $K_d = 1/(K_1K_2)$; thus the value of the equilibrium constant $K_2 = (k_2/k_{-2})$ is 3.8×10^4. From the equilibrium constant K_2 and the rate constant k_2, a value of 0.027 s^{-1} is calculated for k_{-2}, the rate constant for the thermal dissociation of CO from $Fe_{a_3}^{2+}$. This value is in remarkably good agreement with the CO dissociation rate constant of 0.023 s^{-1} previously reported by Greenwood and Gibson (1967).

The activation parameters $\Delta H^\ddagger$ and $\Delta S^\ddagger$ for k_2, the transfer of CO from Cu_B^+ to ferrous cytochrome a_3, can be derived from an Eyring plot (Figure 8). The room temperature point represented by the filled circle is derived from the value of k_2 (1030 s^{-1}) as measured by our UV–vis kinetics studies as a function of [CO]. The other values between 230 and 298 K (open circles with concentric dots and crosses) are observed first-order rate constants for the recombination at 1 atm of CO in the flash photolysis kinetics study reported by Sharrock and Yonetani (1977). The low-temperature points (filled circles, 158–179 K) are from our CO–FTIR studies reported here on the purified enzyme, both in pure aqueous solutions and in 50% glycerol/water solutions. The low-temperature data obtained by others (Fiamingo et al., 1982) by CO–FTIR on mitochondria are shown for comparison (open circles). There is good agreement between the points obtained for the solubilized preparations and for the mitochondria, suggesting that only minor perturbations of the enzyme's active site occur upon removal of the enzyme from the mitochondrial membrane. Moreover, the low-temperature points extrapolate well to the value of k_2, 1030 s^{-1} at room temperature, indicating insignificant change in activation enthalpy with respect to temperature; i.e., $\Delta C_p^\ddagger \approx 0$. The activation parameters for k_2, $\Delta H^\ddagger = 10.0$ kcal mol^{-1} and $\Delta S^\ddagger = -12.0$ cal mol^{-1} deg^{-1}, are among the most precise known being derived from rate constants measured over a temperature range from 140 to 300 K. We note that the negative activation entropy is inconsistent with Cu–CO bond dissociation as the activation step for transfer of CO from Cu to Fe.

Below 260 K the data of Sharrock and Yonetani (1977) follow the same activation plot as our data and those of

Fiamingo et al. (1982), but above 260 K their data deviate from the linear Eyring plot (Figure 8, crosses). These authors' interpretation (Sharrock & Yonetani, 1977) of this deviation was the first partial and then complete melting of the protein surroundings occurs, even at temperatures well below the macroscopic freezing point of the aqueous solution. In our view this interpretation is essentially correct, but because of our results this can be interpreted in more detail as the onset of equilibration of CO between the partially melted protein surroundings and the Cu_B^+–CO complex. Below 260 K the magnitude of the preequilibrium constant K_1 is irrelevant because Cu_B^+–CO does not equilibrate with its solution surroundings under the thoroughly frozen conditions, and the observed rate constant for the rebinding of CO to $Fe_{a_3}^{2+}$ is simply k_2. Between 260 and 273 K the observed rate constant for CO rebinding to cytochrome a_3 starts to decrease as the equilibrium between Cu_B^+–CO and CO in the protein surroundings begins to assert itself kinetically; under these conditions the measured rate constant is intermediate between k_2 and the k_{obs} ($\approx k_2K_1$[CO]), typical of fluid solution. Above 273 K the preequilibrium between the CO in solution and the Cu_B^+–CO complex is fully effective, and the experimentally measured rate constant for the rebinding is k_{obs}.

The Role of Cu_B^+ and the Ligand Shuttle in Cytochrome Oxidase Dynamics. Our results establish that upon photodissociation from cytochrome a_3 at room temperature CO (a) first binds quantitatively to Cu_B^+, (b) rapidly equilibrates with CO in solution, and (c) slowly rebinds to the ferrous cytochrome a_3 from the Cu_B^+–CO complex. If, as we suggest here, the rebinding of CO proceeds via a preequilibrium with Cu_B–CO as an obligatory intermediate species, it should be possible at high [CO] to enter the reversible kinetics regime where the apparent value of k_{-1} (k_{app}) becomes dependent upon [CO] (i.e., $k_{app} = k_{-1} + k_1$[CO], where k_1[CO] is significant compared to k_{-1}). We have recently observed that reversible kinetics indeed occur at high [CO], confirming the preequilibrium suggestion. We emphasize that we find no evidence for a direct pathway from CO in solution to $Fe_{a_3}^{2+}$–CO. As noted earlier, quite recent results (Blackmore et al., 1991; Oliveberg & Malmström, 1992) support our contention that this type of mechanism also applies to the binding of O_2 at the active site.

The TRIR kinetics data make it clear that the direct rebinding of CO to $Fe_{a_3}^{2+}$ following photodissociation is blocked, with the obligatory path for CO being the initial binding to Cu_B^+ (represented by k_3) and subsequent dissociation into solution (k_{-1}). The first step of this process can be understood as simple kinetic control, as discussed in a previous section. Geminate recombination to the heme is, in general, relatively slow (nanoseconds or longer) (Martin et al., 1983), while no such barrier exists to the binding of CO to Cu_B^+, which occurs in less than 1 ps. Therefore, beginning with geminate photodissociated CO, the latter reaction occurs many times faster than the former, and net geminate recombination is not observed.

It is more difficult to understand, however, why CO does not rebind to $Fe_{a_3}^{2+}$ at the same rate at which it dissociates from Cu_B^+. We have shown that Cu_B^+–CO dissociates with a half-life of ca. 1 μs; the barrier to rebinding of CO to $Fe_{a_3}^{2+}$ is expected to be insignificant by comparison. However, we cannot detect any transfer of CO from Cu_B^+ to $Fe_{a_3}^{2+}$ on the time scale of Cu_B^+–CO dissociation. It therefore appears that, subsequent to the fast formation of Cu_B^+–CO, the protein has erected a kinetic barrier to the return of CO to $Fe_{a_3}^{2+}$. Consequently, in the rebinding kinetics, the rate-determining step for the transfer of CO from Cu_B^+ to $Fe_{a_3}^{2+}$ is neither the loss of CO by copper (1–2 μs) nor the intrinsic rate of binding to high-spin ferrous heme (nanosecond time scale) but the surmounting of this kinetic barrier (1030 s^{-1}, 0.7 ms).

The Ligand Shuttle and Its Possible Functional Significance. The reasons why cytochrome oxidase might possess the mechanistic feature inferred in the foregoing discussion deserve examination. A clue as to its nature is found in the fast UV–vis is spectral changes following photodissociation of CO. The binding of CO to Cu_B^+ following photodissociation is followed by a substantial and fast (6 ps) increase in intensity of the α-band of cytochrome a_3; the intensity change reverses within microseconds, as the CO dissociates into solution. These observations as well as the TRIR results for the temporally related Cu–CO and Fe–CO absorbances are summarized in Figure 9, which shows the absorbance changes over 12 orders of magnitude of time. It is most unlikely that the substantial spectral changes in the α-band are caused simply by the binding of CO to Cu_B^+, nor are the reverse changes likely to be simply due to the departure of CO from the cuprous center. Rather, they are more likely to result from significant structural changes at the cytochrome a_3 heme itself.

We suggest that this structural change consists of the transfer of a ligand (L) from Cu_B to Fe_{a_3}, triggered by the binding of CO to Cu_B, with attendant changes in coordination and electronic spectrum of the heme. The transferred ligand occupies the former CO binding site on the heme and prevents return of CO until the Fe–L bond breaks. This suggestion is supported by the spectral changes themselves and by the slow rate of transfer of CO from Cu_B to Fe_{a_3} (1030 s^{-1}, which in this scenario is the thermal Fe–L bond scission rate). It is even more strongly supported by our observation that the formation of Fe_{a_3}–CO, which is itself photolabile, is accelerated by light. This occurs even at the relatively low probe light levels present in the kinetic spectrophotometer (as noted earlier) and can be made quite substantial by illuminating the CcO/CO sample with continuous-wave laser light during the rebinding reaction (R. B. Dyer, unpublished observation). In our view this occurs because the proposed Fe–L intermediate is photolabile; consequently, illumination during rebinding increases the rate of Fe–L bond scission and thereby both k_2 and k_{obs}.

We now turn our attention to the detailed axial ligation options open to the transient structure wherein L is transferred from Cu_B to Fe_{a_3}. There are three obvious possibilities for the state of cytochrome a_3 after ligand transfer; (i) the heme may be six-coordinate and low spin; (ii) it may be six-coordinate and high spin; and (iii) it may be five-coordianate and high spin with L occupying the distal (CO binding) coordination site and the proximal histidine imidazole displaced. The first possibility is easily dismissed because time-resolved magnetic circular dichroism data clearly show that the cytochrome a_3 species is high spin on all time scales following photodissociation (Woodruff et al., 1991; Goldbeck et al., 1991). The participation of a six-coordinate high-spin species appears most unlikely for the following reasons. First, no known six-coordinate high-spin ferrous heme or porphyrin model complex exists with imidazole as one of the axial ligands. Second, typical ligand-exchange rate constants for six-coordinate high-spin ferrous complexes are ca. 10^5–10^6 s^{-1} (Eigen & Wilkins, 1965), 2–3 orders of magnitude faster than the rate of 1030 s^{-1} that we observe for Fe–L bond scission. On the other hand, Dixon and co-workers (Shirazi et al., 1985) have shown that imidazole-exchange rate constants of high-spin five-coordinate ferrous heme imidazole model complexes are near 1500 s^{-1} in nonpolar solvents. This is the remaining possibility for the Fe–L transient, namely, that it is a high-spin five-

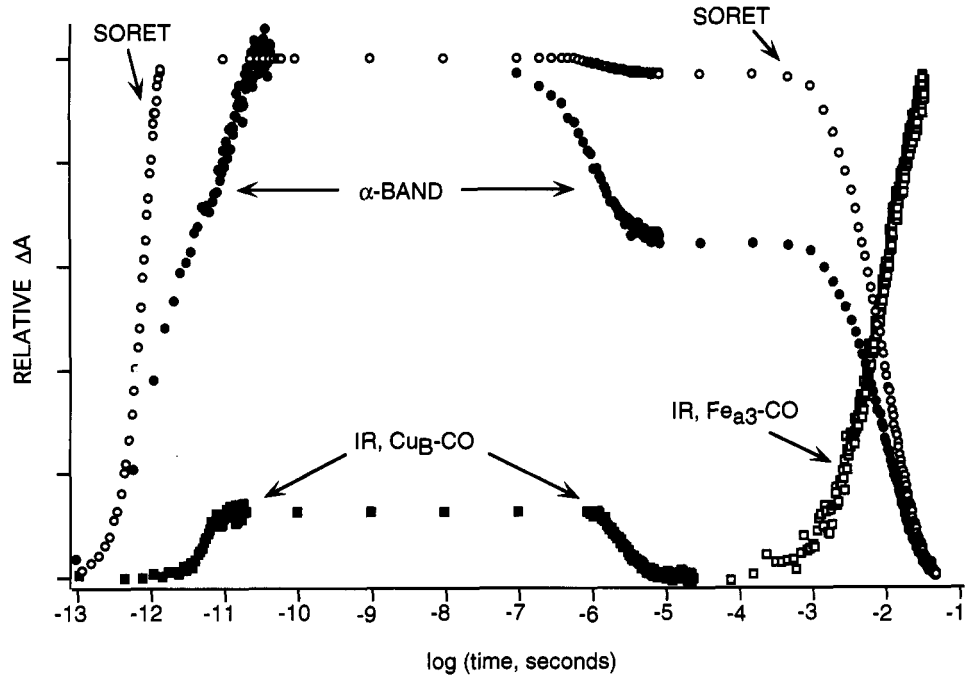

FIGURE 9: Log(time) plot of the electronic and infrared absorbance changes following photodissociation of CO–cytochrome oxidase. Open and filled circles represent electronic absorbance data taken in the Soret and α-band regions, respectively. Filled squares correspond to infrared absorbance of the Cu_B–CO complex (2062 cm^{-1}), and open squares denote the return of infrared absorbance due to the Fe_{a_3}–CO complex (1963 cm^{-1}).

coordinate ferrous species in which L is coordinated to the (distal) CO-binding site and the original proximal histidine is displaced. This structure for the transient is consistent with the facts developed in this study and discussed above and elsewhere (Woodruff et al., 1991a) and with the stablished behavior of analogous proteins and model systems.

The binding of CO to Cu_B on its path to and from cytochrome a_3 provides an explanation for the relatively slow kinetics of CO rebinding to cytochrome a_3 in cytochrome oxidase as compared to Hb (Martin et al., 1983). This, in turn, suggests that the protein has a means of directing incoming ligands to Cu_B rather than to cytochrome a_3. The recent results of Blackmore et al. (1991) as well as those of Oliveberg and Malmström (1992) may be taken as strong evidence that this occurs not only for CO but for O_2 as well, and thus, we infer that this mechanistic feature of CcO is both general and functionally significant. Most simply, the spatial orientation of Cu_B^+ and $Fe_{a_3}^{2+}$ with respect to incoming ligands is such that the incoming molecule first encounters the copper as it diffuses to the binuclear center; this scenario is depicted in Figure 10, species **1** and **2**. In more general terms, this binding of exogenous ligands (particularly O_2) to copper could serve as a gating mechanism for the overall function of the enzyme and may be relevant to its regulation of the physiological activity of CcO.

The identity of the endogenous ligand L is unknown, but our results give us some information regarding its nature. It appears that the binding of L to the heme is more favorable than the binding of the proximal histidine when the CO is bound to Cu_B. The steric and electronic properties of this ligand must trigger breaking the proximal Fe–His bond when L binds on the distal size. We have previously discussed (Woodruff et al., 1991a) possible candidates for L. A few amino acid side chains in addition to His-Im as well as deprotonated peptide nitrogen might satisfy the rather restrictive criteria for L. We also suggested that the unsaturated farnesyl side chain of heme *a*, bound to Cu_B as olefin and to Fe_{a_3} as allyl, might be a reasonable candidate for L. In any case, it may be a common phenomenon that the binding and dissociation of exogenous ligands (CO, NO, and, most importantly, O_2) at Cu_B^+ induces the transfer of an endogenous ligand between Cu_B and cytochrome a_3 with the simultaneous release and rebinding of the proximal histidine. These pheneomena and associated protonation/deprotonation reactions could act as microscopic "gates" in the proton-translocation mechanism of cytochrome oxidase.

It is clear that the net free energy necessary to accomplish proton translocation against an ion gradient must come from the electron-transfer reaction between O_2 and cytochrome *c* which is catalyzed by the enzyme. However, the free energies associated with the ligation reactions are comparable to the electron-transfer processes within cytochrome oxidase (e.g., the binding of CO to Fe_{a_3} has a free energy equivalent to 384 mV). The ligation reactions must be considered to be energetically competent to participate in proton translocation despite the fact that they represent (as do the internal electron-transfer reactions) closed cycles in the catalytic process. Thus we envision that the exchange of ligands between the Cu_B and $Fe_{a_3}^{2+}$ may gate proton access to the redox centers and couple changes in the free energy of their oxidation–reduction cycle to the translocation of protons. Elsewhere (Woodruff et al., 1991a–c; Woodruff, 1993) we offer more detailed speculations as to how this might occur. Moreover, there are clear experimental presciptions for testing these speculations.

CONCLUSIONS

We have shown that the obligatory path of CO to and from the cytochrome a_3 of cytochrome oxidase involves transient binding of CO to Cu_B^+ as indicated in Scheme I. We have measured experimentally or can calculate the value of every rate and equilibrium constant in Scheme I, and these are summarized in Table I. We note that k_2 calculated from K_2 and k_2 is 0.027 s^{-1}. This is in remarkably good agreement with the measured value (Greenwood & Gibson, 1967) of 0.023 s^{-1}. We take this agreement to be very strong evidence for the validity of Scheme I in accounting for the general mechanistic features of ligand binding to CcO.

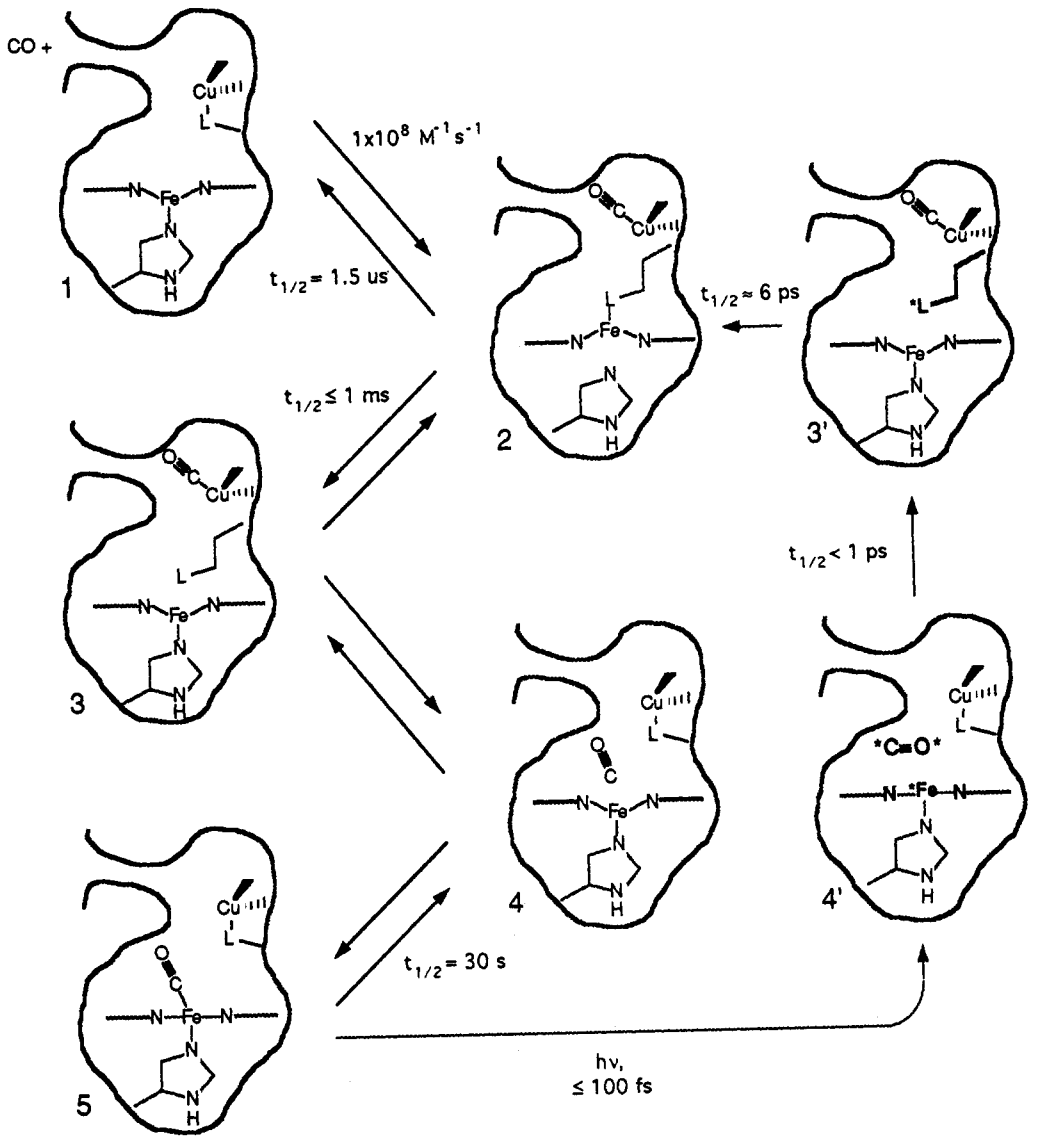

FIGURE 10: Schematic representation of the proposed minimal mechanism for the photodissociation and rebinding of CO in fully reduced cytochrome oxidase. See text.

Table I: Rate and Equilibrium Constants for CcO–CO Photodissociation and Rebinding

constant (see Scheme I)	measured value[a]	calculated[a]
K_1 (M^{-1})	87	
k_1 (M^{-1} s^{-1})		6.8×10^7
k_{-1} (s^{-1})	4.7×10^5 (IR)[b]	
	7.9×10^5 (UV–vis)	
K_2		3.8×10^4
k_2 (s^{-1})	1030	
k_{-2} (s^{-1})	0.023[c]	0.027
k_3 (s^{-1})	$>7 \times 10^{11}$ [d]	

[a] Present work unless otherwise referenced. [b] Dyer et al., 1989a. [c] Greenwood & Gibson, 1967. [d] Dyer et al., 1991.

Significant microscopic details are missing from Scheme I, however. In particular, this scheme does not account for the picosecond and microsecond changes in the α-band absorbance, the fact that k_2 is 1000 times smaller than k_{-1}, and the observed photoacceleration of the rebinding of CO to CcO. The full "ligand shuttle" mechanism depicted in Figure 10 and discussed in detail elsewhere (Woodruff et al., 1991a) is needed to accommodate these facts. We suggest that the binding of CO to Cu_B triggers the transfer of an endogenous ligand from Cu_B^+ to the heme and that this process is reversed when CO dissociates from Cu_B^+. These processes appear to be accompanied by the breaking and re-formation of the proximal histidine bond. Thus the binding of CO to Cu_B results in a five-coordinate high-spin cytochrome a_3 transient (Woodruff et al., 1991a; Goldbeck et al., 1991). The dissociation (thermal or photoactivated) of the endogenous ligand from the heme is the rate-determining step for the return of CO from Cu_B to its thermodynamically stable site on the heme. We suggest here and elsewhere (Woodruff et al., 1991a–c; present work), with significant new experimental support (Blackmore et al., 1991; Oliveberg & Malmström, 1992), that the binding of small exogenous ligands, including O_2, to Cu_B^+ and the attendant ligand shuttle may be general features of cytochrome oxidase reactivity. Furthermore, we note the similarity of the rate of rebinding of photolyzed CO to cytochrome a_3 (1030 s^{-1}), and also the activation parameters, to those of the photoinduced electron-transfer reaction in the mixed-valence enzyme (Brzezinski & Malmström, 1987; Malmström, 1990). This suggests that the same process (namely, Fe–L bond scission) may control the rates of both processes. We note that it is common in inorganic chemistry for both the rates and the energetics of electron-transfer reactions to be exquisitely sensitive to the coordination chemistry of the metal centers involved. It is also common for the protonation state of a ligand to be affected by whether it is coordinated to a metal ion and, if it is coordinated, to the oxidation state of the metal. Thereby, coordination chemistry offers an established

mechanism in small-molecule chemistry for coupling redox and proton-transfer reactions. Finally, we note that it is possible to envision that directed protonation/deprotonation reactions of the ligands may accompany the coordination reactions shown in Figure 10 (Woodruff et al., 1991b,c), as well as the redox reactions in the functional cycle of the enzyme. Thus the ligand shuttle potentially offers a reasonable mechanism for coupling redox reactivity to proton translocation. In view of these circumstances, serious consideration must be given to the possible generality and functional significance of the ligand shuttle. Studies addressing these issues are in progress, and specific microscopic mechanisms for the control and coupling of electron transfer and protein translocation are discussed elsewhere (Woodruff, 1993).

REFERENCES

Alben, J. O., Moh, P. P., Fiamingo, F. G., & Altschuld, R. A. (1981) *Proc. Natl. Acad. Sci. U.S.A. 78*, 234–237.

Atherton, S. J., Hubig, S. M., Callan, T. J., Duncanson, J. A., Snowden, P. T., & Rodgers, M. A. J. (1987) *J. Phys. Chem. 91*, 3137–3140.

Austin, R. H., Beeson, K. W., Eisenstein, L., Frauenfelder, H., & Gunsalus, I. C. (1975) *Biochemistry 14*, 5355–5373.

Babcock, G. T. (1988) in *Biological Applications of Raman Spectroscopy* (Spiro, T. G., Ed.) Vol. 3, p 298, Wiley-Interscience, New York.

Babcock, G. T., Jean, J. M., Johnston, L. N., Palmer, G. W., & Woodruff, W. H. (1984) *J. Am. Chem. Soc. 106*, 8305–8306.

Baker, G. M., Noguchi, M., & Palmer, G. (1987) *J. Biol. Chem. 262*, 595–604.

Blackmore, R. S., Greenwood, C., & Gibson, Q. H. (1991) *J. Biol. Chem. 266*, 19245–19249.

Boelens, R., Rademaker, H., Wever, R., & Van Gelder, B. F. (1984) *Biochim. Biophys. Acta 765*, 196–209.

Bombelka, E., Richter, F.-W., Stroh, A., & Kadenbach, B. (1986) *Biochem. Biophys. Res. Commun. 140*, 1007–1014.

Brzezinski, P., & Malmström, B. G. (1987) *Biochim. Biophys. Acta 894*, 29–38.

Caughey, W. S. (1980) in *Methods for Determining Metal Ion Environments in Proteins: Structure and Function of Metalloproteins* (Darnall, D. W., & Wilkins, R. G., Eds.) pp 95–115, Elsevier/North-Holland, New York.

Chance, B., Saronio, C., & Leigh, J. S., Jr. (1975) *J. Biol. Chem. 250*, 9226–9237.

Choc, M. G., & Caughey, W. S. (1981) *J. Biol. Chem. 256*, 1831–1838.

Clore, G. M., Andréasson, L.-E., Karlsson, B., Aasa, R., & Malmström, B. G. (1980) *Biochem. J. 185*, 139–145.

Dyer, R. B., Einarsdóttir, Ó., Killough, P. M., López-Garriga, J. J., & Woodruff, W. H. (1989a) *J. Am. Chem. Soc. 111*, 7657–7659.

Dyer, R. B., López-Garriga, J. J., Einarsdóttir, Ó., & Woodruff, W. H. (1989b) *J. Am. Chem. Soc. 111*, 8963–8963.

Dyer, R. B., Peterson, K. A., Stoutland, P. O., & Woodruff, W. H. (1991) *J. Am. Chem. Soc. 113*, 6276–6277.

Eigen, M., & Wilkins, R. G. (1965) *Adv. Chem. Ser. 49*, 55–80.

Einarsdóttir, Ó., & Caughey, W. S. (1985) *Biochem. Biophys. Res. Commun. 129*, 840–847.

Einarsdóttir, Ó., Choc, M. G., Weldon, S., & Caughey, W. S. (1988) *J. Biol. Chem. 263*, 13641–13654.

Einarsdóttir, Ó., Killough, P. M., Fee, J. A., & Woodruff, W. H. (1989) *J. Biol. Chem. 264*, 2405–2408.

Fager, L. Y., & Alben, J. O. (1972) *Biochemistry 11*, 4786–4792.

Fiamingo, F. G., Altschuld, R. A., Moh, P. P., & Alben, J. O. (1982) *J. Biol. Chem. 257*, 1639–1650.

Findsen, E. W., Centeno, J., Babcock, G. T., & Ondrias, M. R. (1987) *J. Am. Chem. Soc. 109*, 5367–5372.

Gibson, Q. H., & Greenwood, C. (1963) *Biochem. J. 86*, 541–554.

Goldbeck, R. A., Dawes, T. D., Einarsdóttir Ó., Woodruff, W. H., & Kliger, D. S. (1991) *Biophys. J. 60*, 125–134.

Greenwood, C., & Gibson, Q. H. (1967) *J. Biol. Chem. 242*, 1782–1787.

Hill, B. C., Greenwood, C., & Nicholls, P. (1986) *Biochim. Biophys. Acta 853*, 91–113.

Karlsson, B., Aasa, R., Vänngård, T., & Malmström, B. G. (1981) *FEBS Lett. 131*, 186–188.

Keilin, D., & Hartree, E. F. (1938) *Nature 141*, 870–871.

Kronek, P. M. H., Zumft, W. G., Kastrau, D. W. H., Riester, J., & Antholine, W. E. (1991) *J. Inorg. Biochem. 43*, 164.

Malmström, B. G. (1990) *Chem. Rev. 90*, 1247–1260.

Martin, J.-L., Migus, A., Poyart, C., Lecarpentier, Y., Astier, R., & Antonetti, A. (1983) *Proc. Natl. Acad. Sci. U.S.A. 80*, 173–178.

Oliveberg, M., & Malmström, B. G. (1992) *Biochemistry 31*, 3560–3563.

Sharrock, M., & Yonetani, T. (1977) *Biochim. Biophys. Acta 462*, 718–730.

Shimada, H., & Caughey, W. S. (1982) *J. Biol. Chem. 257*, 11893–11900.

Shirazi, A., Barbush, M., Ghosh, S., & Dixon, D. W. (1985) *Inorg. Chem. 24*, 2495–2502.

Song, S., Hua, S., Ching, Y., & Rousseau, D. (1992) *Biophys. J. 61*, A202.

Steffans, G. C. M., Biewald, R., & Buse, G. (1987) *Eur. J. Biochem. 164*, 295–300.

Stevens, T. H., Brudvig, G. W., Bocian, D. F., & Chan, S. I. (1979) *Proc. Natl. Acad. Sci. U.S.A. 76*, 3320–3324.

Stoutland, P. O., Lambry, J.-C., Martin, J.-L., & Woodruff, W. H. (1991) *J. Phys. Chem. 95*, 6406–6408.

Wikström, M., Krab, K., & Saraste, M. (1981) *Cytochrome Oxidase-A Synthesis*, Academic Press, New York.

Woodruff, W. H. (1993) *J. Bioenerg. Biomembr.* (in press).

Woodruff, W. H., Einarsdóttir Ó., Dyer, R. B., Bagley, K. A., Palmer, G., Atherton, S. J., Goldbeck, R. J., Dawes, T. D., & Kliger, D. S. (1991a) *Proc. Natl. Acad. Sci. U.S.A. 82*, 2588–2592.

Woodruff, W. H., Dyer, R. B., Einarsdóttir, Ó., Peterson, K. A., Stoutland, P. O., Bagley, K. A., Palmer, G., Schoonover, J. R., Kliger, D. S., Goldbeck, R. J., Dawes, T. D., Martin, J.-L., Lambry, J.-C., Atherton, S. J., & Hubig, S. M. (1991b) *Proc. SPIE–Int. Soc. Opt. Eng. 1432*, 205–210.

Woodruff, W. H., Dyer, R. B., Einarsdóttir, Ó., Peterson, K. A., Stoutland, P. O., Bagley, K. A., Palmer, G., Schoonover, J. R., Kliger, D. S., Goldbeck, R. J., Dawes, T. D., Martin, J.-L., Lambry, J.-C., Atherton, S. J., & Hubig, S. M. (1991c) in *Spectroscopy of Biological Molecules* (Hester, R. E., & Girling, R. B., Eds.) pp 235–238, Royal Society of Chemistry, Cambridge.

Woodruff, W. H., Dyer, R. B., & Einarsdóttir, Ó. (1993) in *Biomolecular Spectroscopy* (Clark, R. J. H., & Hester, R. E., Eds.) Part B, pp 189–233, Jon Wiley and Sons Ltd., New York.

Yoshikawa, S., & Caughey, W. S. (1982) *J. Biol. Chem. 257*, 412–420.

Yoshikawa, S., & Caughey, W. S. (1990) *J. Biol. Chem. 265*, 7945–7958.

Yoshikawa, S., Choc, M. G., O'Toole, M. C., & Caughey, W. S. (1977) *J. Biol. Chem. 252*, 5498–5508.